Support information

High Performance Pd_xCu_y Bimetal Catalysts With Adjustable Faraday Current Efficiency for Nitrogen Fixation

Hongxi Zhang[a,b], Zengyao Wang[a,b], Jianfeng Shen[a], Mingxin Ye[a]**

[a] Institute of special materials and technology, Fudan University, Shanghai 200433, China

[b] Department of Chemistry, Fudan University, Shanghai 200433, China

E-mail: mxye@fudan.edu.cn, jfshen@fudan.edu.cn

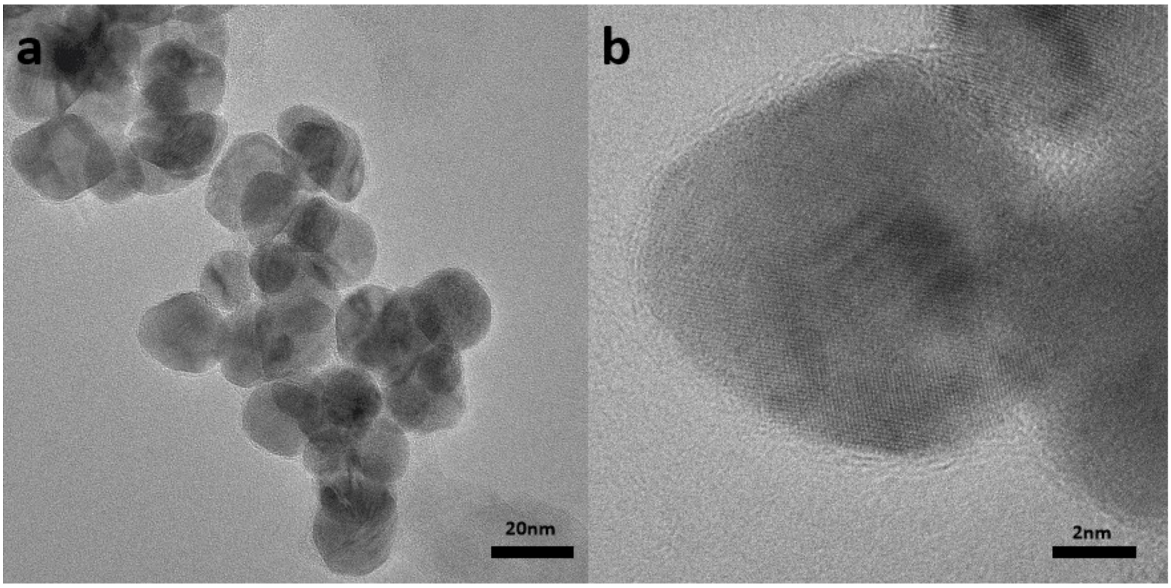

Figure S1.(a,b) TEM images of PdCu.

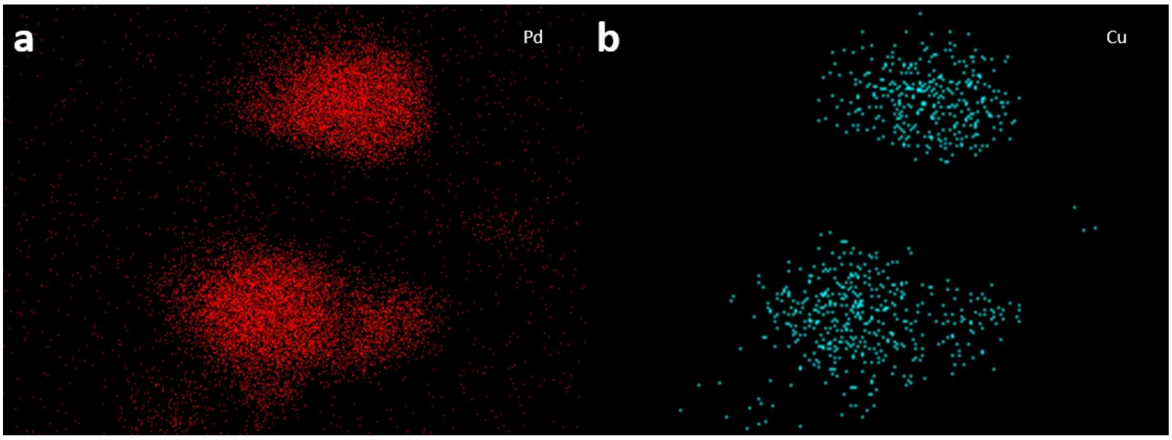

Figure S2.(a,b) TEM-EDS mapping of PdCu.

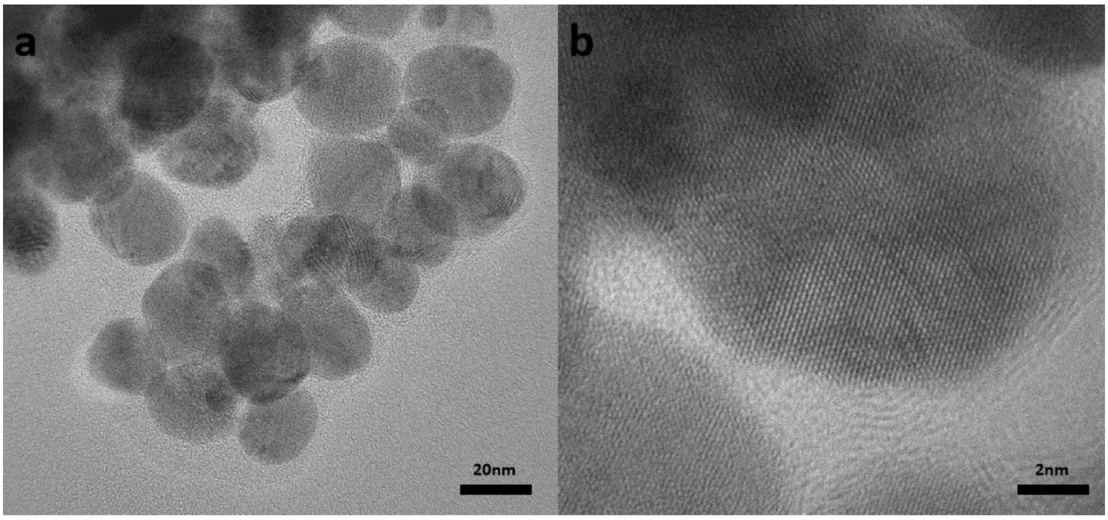

Figure S3. (a,b) TEM image of Pd_3Cu.

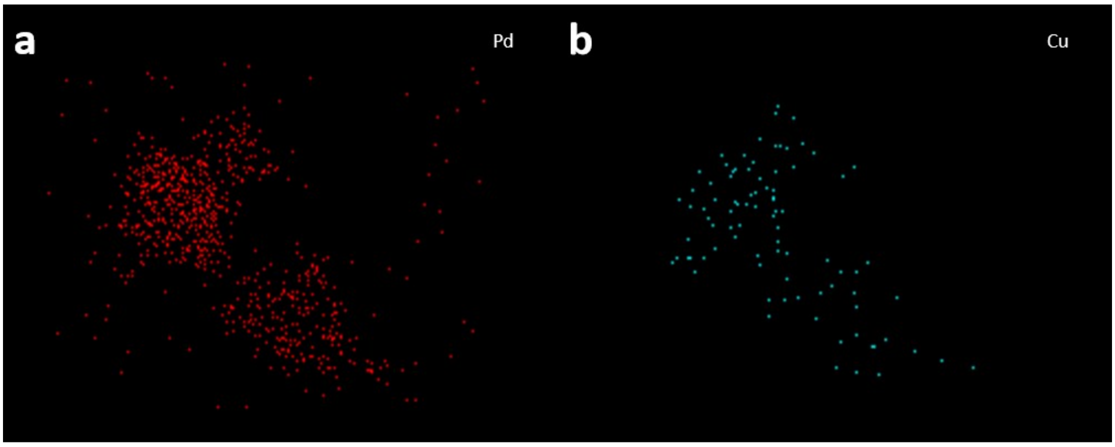

Figure S4.(a,b) TEM-EDS mapping of Pd_3Cu.

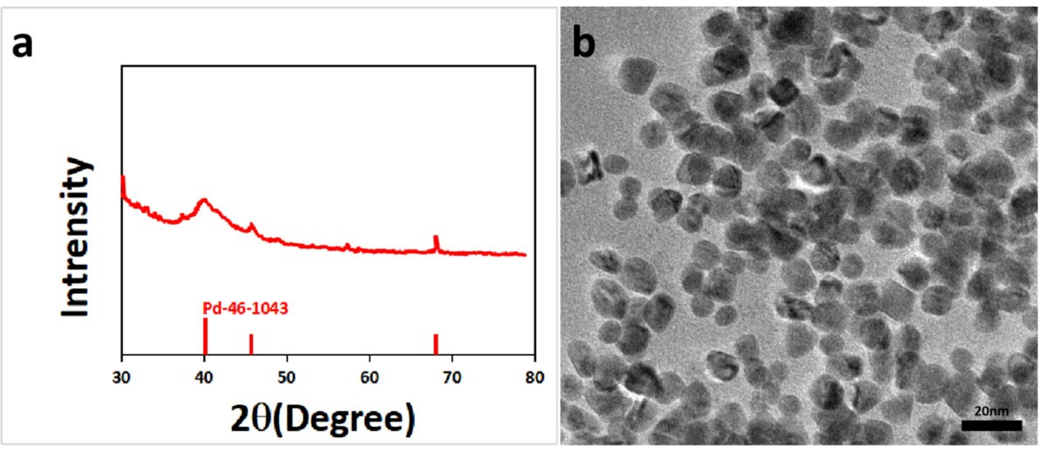

Figure S5. (a) XRD pattern and (b) TEM image of Pd.

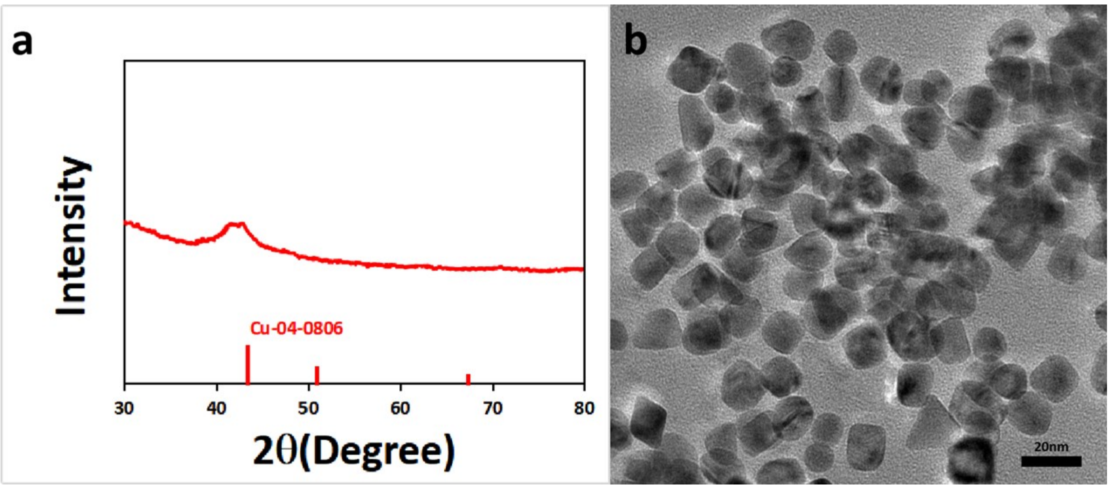

Figure S6.(a) XRD pattern and (b) TEM image of Cu.

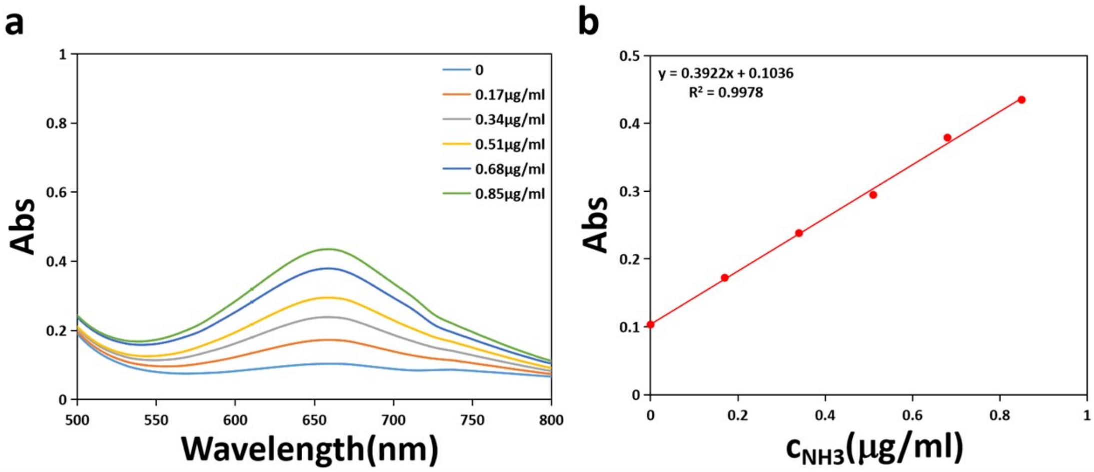

Figure S7.(a) UV-Vis curves of indophenol assays with NH_4^+ ions after incubated for 1 h at room temperature. (b) Calibration curve used for estimation of NH_3 by NH_4^+ ion concentration. The fitting curve shows good linear relation of absorbance with NH_4^+ ion concentration (y = 0.3922x + 0.1036, R^2=0.9978) for three independent calibration curves.

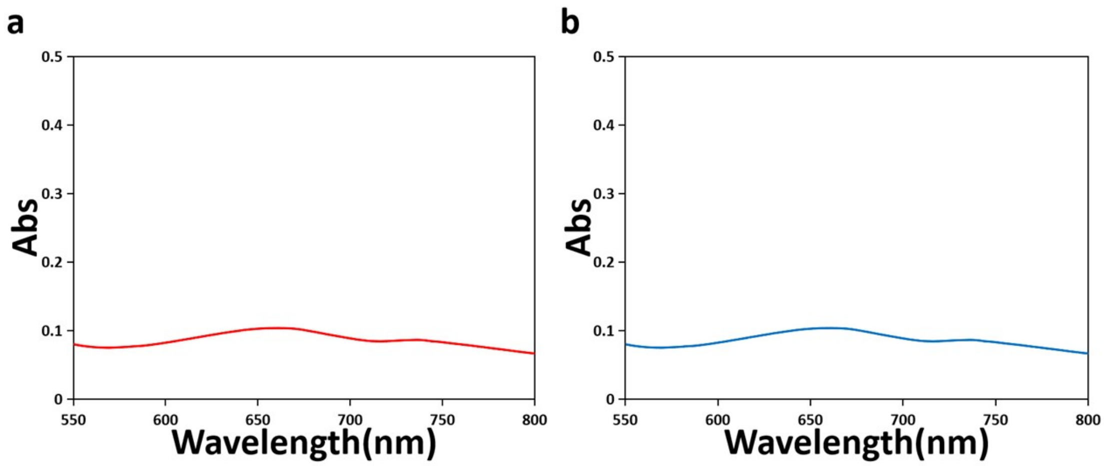

Figure S8. (a)UV-vis spectra of 0.1M HCl and (b) after 2h reaction with Ar by the indoxyl blue method.

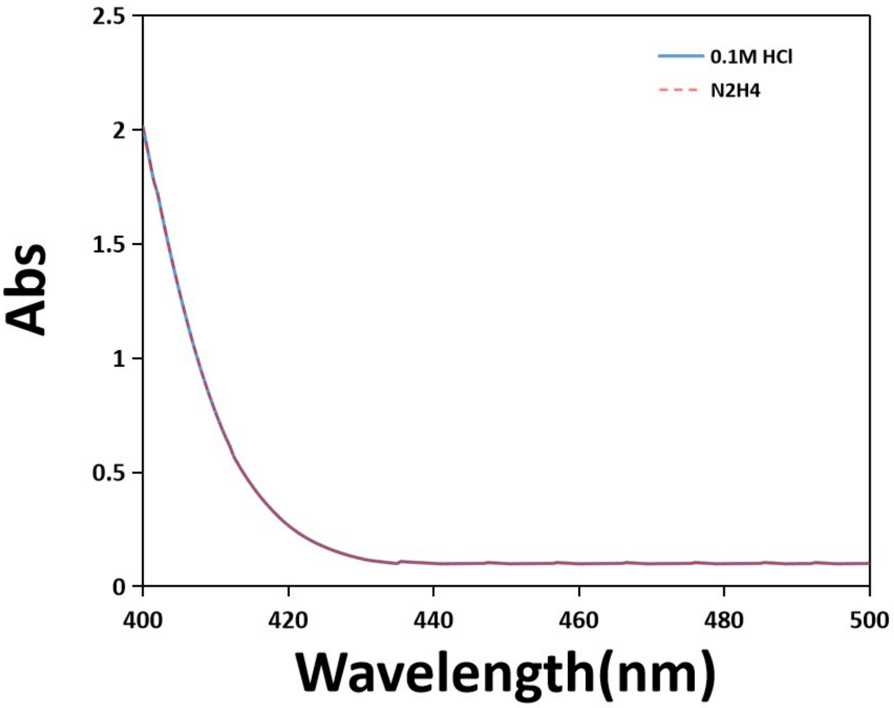

Figure S9. UV-vis spectrum for the potential by-product N_2H_4.

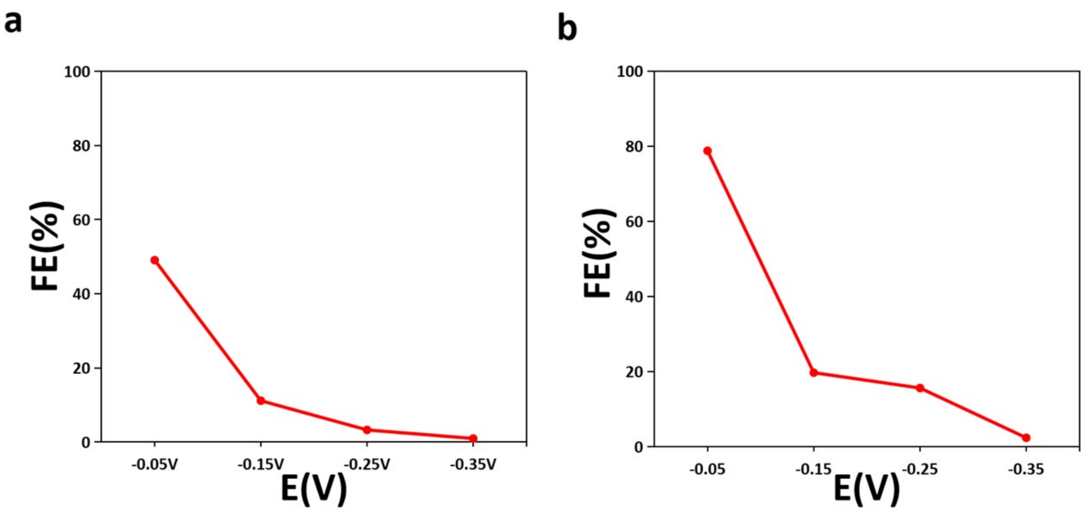

Figure S10.(a) FE of Pd_3Cu and (b) $PdCu_3$.

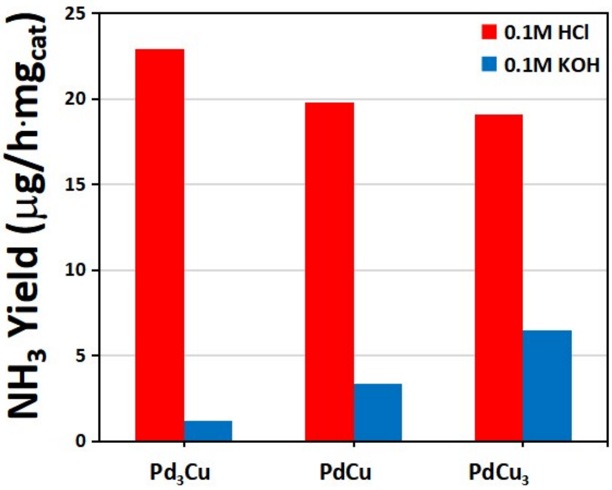

Figure S11. NH_3 yields of Pd_xCu_y at 0.1M HCl and 0.1M KOH.

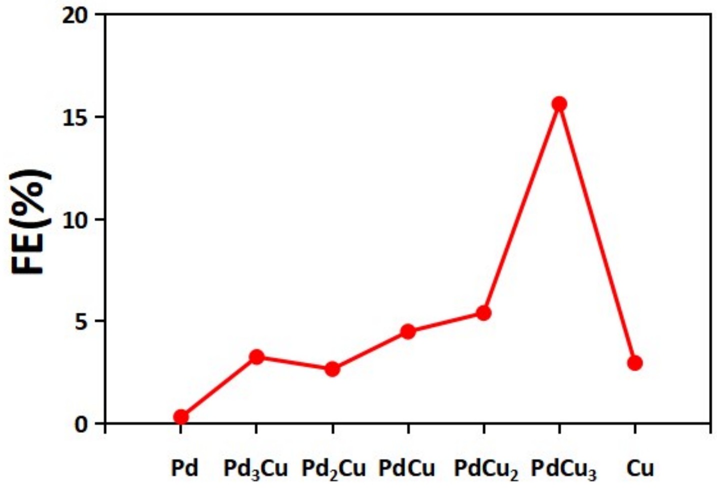

Figure S12. FE of Pd_xCu_y with more Pd/Cu atom ratio.

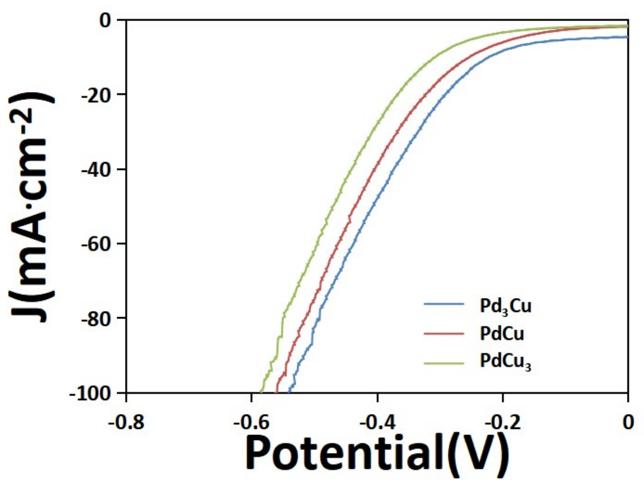

Figure S13. LSV curves of Pd_3Cu, PdCu and $PdCu_3$ bimetal catalysts in 0.05M H_2SO_4.

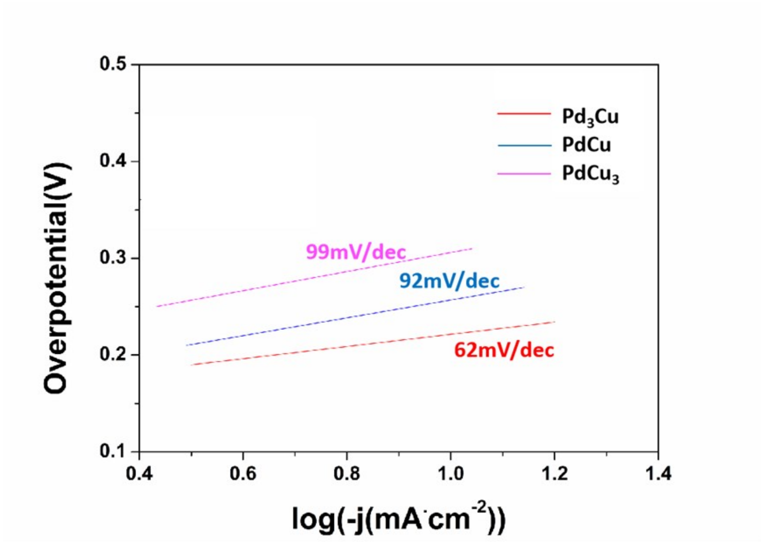

Figure S14. Tafel plots at -0.25V vs RHE. of Pd_3Cu, PdCu and $PdCu_3$ bimetal catalysts in 0.05M H_2SO_4.

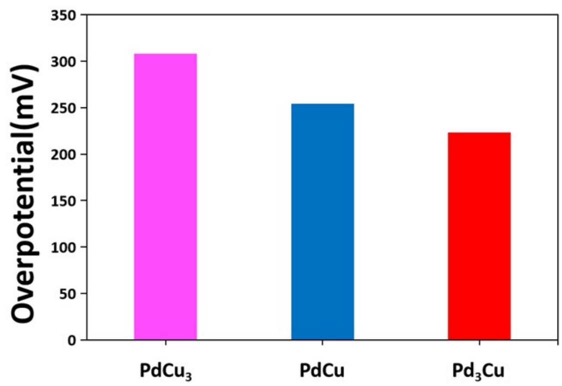

Figure S15. Overpotential of Pd_3Cu, PdCu and $PdCu_3$ bimetal catalysts at 10 $mA \cdot cm^{-2}$ in 0.05M H_2SO_4.

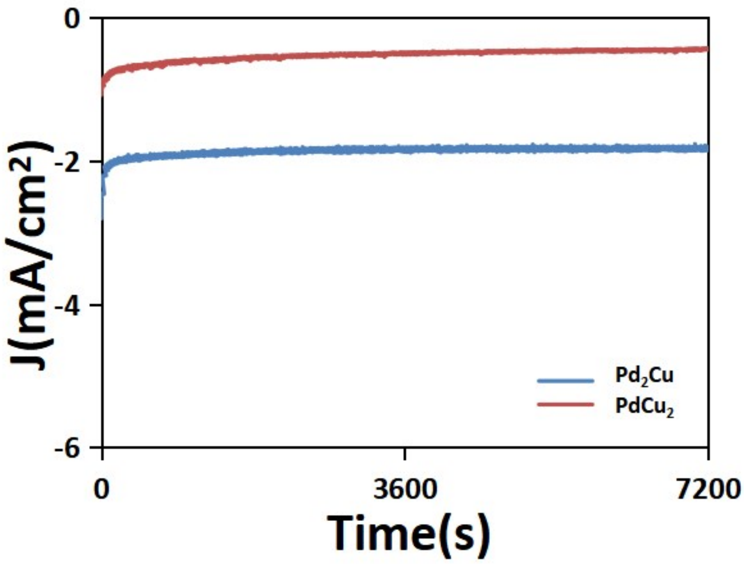

Figure S16. i-t curves at -0.25V vs. RHE. of Pd_2Cu and $PdCu_2$.

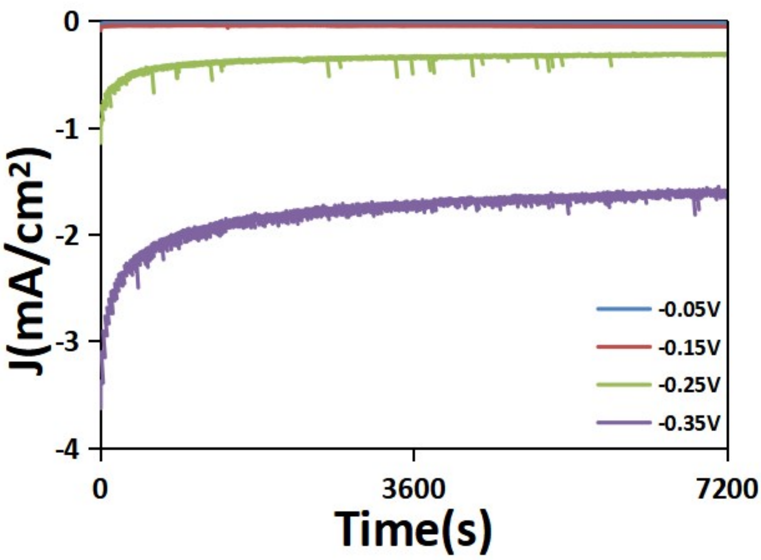

Figure S17. i-t curves of $PdCu_3$ at different potentials.

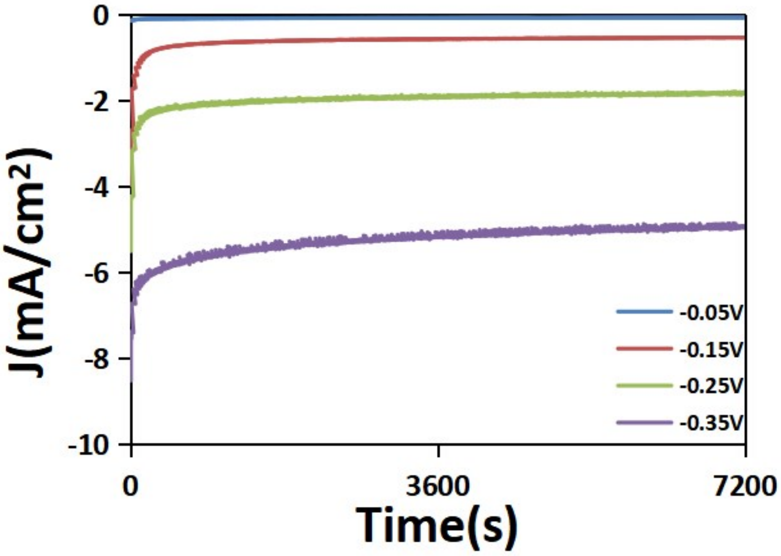

Figure S18. i-t curves at different potentials of Pd_3Cu.

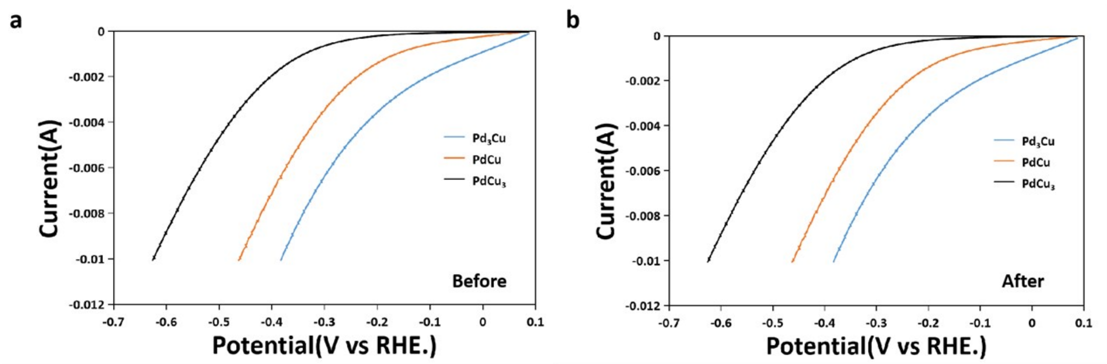

Figure S19. (a)LSV curves of Pd_3Cu, PdCu and $PdCu_3$ bimetal catalysts before NRR test and (b) LSV curves after NRR test.

Table S1. NH_3 yield and FE of different materials

Catalysts	Electrolyte	Yield/μg·h^{-1}·mg$^{-1}_{cat}$	FE/%	Ref.
$PdCu_3$ nanoparticles	0.1 M HCl	19.1	15.62	This work
Flower-like Au	0.1 M HCl	25.57	6.05	*ACV MATER* 2017, **29**, 1700001
Au/CeOx-RGO	0.1 M HCl	8.3	10.1	*CHEMSUSCHEM*, 2018, **11**, 3480-3485.
$Bi_4V_2O_{11}$-CeO_2	0.1 M HCl	23.21	10.16	*SMALL METHODS*, 2018, **3**, 1800333.
CoO/RGO	0.1 M Na_2SO_4	21.5	8.3	*J MATER CHEM A*, 2019, **7**, 4389-4394.
Hierarchical CoP hollow nanocages	1 M KOH	10.78	7.36	*SMALL METHODS*, 2018, **2**, 1800204.
Cr_2O_3 nanofiber	0.1 M HCl	28.13	8.56	*CHEM COMMUN*, 2018, **54**, 12848-12851.
Cr_2O_3/RGO	0.1 M HCl	33.3	7.33	*INORG CHEM*, 2019, **58**, 2257-2260.
Multishelled hollow Cr_2O_3 microspheres	0.1 M Na_2SO_4	25.3	6.78	*ACS CATAL*, 2018, **8**, 8540-8544.
$Ti_3C_2T_x$ MXene nanosheets	0.1 M HCl	20.4	9.3	*J MATER CHEM A*, 2018, **6**, 24031-24035.
Fe_2O_3 nanorods	0.1 M Na_2SO_4	15.9	0.94	*CHEMCATCHEM*, 2018, **10**, 4530-4535.
β-FeOOH nanorods	0.5 M $LiClO_4$	23.32	6.7	*CHEM COMMUN*, 2018, **54**, 11332-11335.
Nb2O5 nanofiber	0.1 M HCl	43.6	9.26	*NANO ENERGY*, 2018, **52**, 264-270.
Mo_2C-C	0.5 M Li_2SO_4	11.3	7.8	*ADV MATER*, 2018, **30**, 1803694.
Pd-Ru with porous nanostructures	0.1 M HCl	25.92	1.53	*ACS SUSTAIN CHEM ENG*, 2018, **7**, 2400-2405.
Pd-Ru tripods	0.1 M KOH	37.23	1.85	*J MATER CHEM A*, 2019, **7**, 801-805.
PdCuIr	0.1 M Na_2SO_4	13.43	5.29	*J MATER CHEM A*, 2019, **7**, 3190-3196.
Polymeric carbon nitride	0.1 M HCl	8.09	11.59	*ANGEW CHEM INT ED*, 2018, **57**, 10246-10250.